

Suppression of insulin feedback enhances the efficacy of PI3K inhibitors

Benjamin D. Hopkins¹, Chantal Pauli^{2,3}, Xing Du⁴, Diana G. Wang^{1,5}, Xiang Li⁶, David Wu¹, Solomon C. Amadiume¹, Marcus D. Goncalves^{1,7}, Cindy Hodakoski¹, Mark R. Lundquist¹, Rohan Bareja^{1,3,8}, Yan Ma⁴, Emily M. Harris⁴, Andrea Sboner^{1,3,8,9}, Himisha Beltran^{1,3,10}, Mark A. Rubin^{3,11}, Siddhartha Mukherjee^{4*} & Lewis C. Cantley^{1*}

Mutations in PIK3CA, which encodes the p110 α subunit of the insulin-activated phosphatidylinositol-3 kinase (PI3K), and loss of function mutations in PTEN, which encodes a phosphatase that degrades the phosphoinositide lipids generated by PI3K, are among the most frequent events in human cancers^{1,2}. However, pharmacological inhibition of PI3K has resulted in variable clinical responses, raising the possibility of an inherent mechanism of resistance to treatment. As p110 α mediates virtually all cellular responses to insulin, targeted inhibition of this enzyme disrupts glucose metabolism in multiple tissues. For example, blocking insulin signalling promotes glycogen breakdown in the liver and prevents glucose uptake in the skeletal muscle and adipose tissue, resulting in transient hyperglycaemia within a few hours of PI3K inhibition. The effect is usually transient because compensatory insulin release from the pancreas (insulin feedback) restores normal glucose homeostasis³. However, the hyperglycaemia may be exacerbated or prolonged in patients with any degree of insulin resistance and, in these cases, necessitates discontinuation of therapy^{3–6}. We hypothesized that insulin feedback induced by PI3K inhibitors may reactivate the PI3K-mTOR signalling axis in tumours, thereby compromising treatment effectiveness^{7,8}. Here we show, in several model tumours in mice, that systemic glucose-insulin feedback caused by targeted inhibition of this pathway is sufficient to activate PI3K signalling, even in the presence of PI3K inhibitors. This insulin feedback can be prevented using dietary or pharmaceutical approaches, which greatly enhance the efficacy/toxicity ratios of PI3K inhibitors. These findings have direct clinical implications for the multiple p110 α inhibitors that are in clinical trials and provide a way to increase treatment efficacy for patients with many types of tumour.

The relationship between PI3K inhibitors and the disruption of systemic glucose homeostasis has been evident from the beginning of their use in clinical trials³. However, hyperglycaemia has largely been approached as a treatment-related complication that requires management in only a subset of patients for whom it becomes persistent. Owing to the body's normal glycaemic regulation, patients treated with these agents experience some degree of systemic hyperinsulinaemia as the pancreas attempts to normalize serum glucose levels. Because insulin is a potent stimulator of PI3K signalling in tumours and can have profound effects on cancer progression^{9–11}, we hypothesized that the treatment-induced hyperinsulinaemia might limit the therapeutic potential of agents that target the PI3K pathway. To test this theory, we treated wild-type mice with therapeutic doses of compounds targeting a variety of kinases in the insulin receptor-PI3K-mTOR pathway, including inhibitors of IRS1 and IGFR, PI3K, AKT, and mTOR, and

monitored their blood glucose levels over time after treatment (Fig. 1a, Extended Data Fig. 1a, b). As expected, many of these agents caused substantial increases in blood glucose levels. Notably, the hyperglycaemia resolved after only a few hours without additional intervention, suggesting that PI3K signalling had been reactivated in muscle and liver despite the presence of the drug. For each of the agents that caused an increase in blood glucose, there was also an increase in the amount of insulin released into the serum as measured by enzyme-linked immunosorbent assays (ELISAs) for insulin over time (Fig. 1b) and c-peptide, which is clinically used as a surrogate for insulin over time^{12–14} (Fig. 1c, Extended Data Fig. 1c, d). To assess whether these PI3K inhibitor-induced spikes in glucose and insulin affected tumours, we performed fluorodeoxyglucose positron emission tomography (FDG-PET) on mice bearing orthotopic Kras-Tp53-Pdx-Cre (KPC) tumour allografts in the pancreas¹⁵. We observed an increase in glucose uptake in these tumours 90 min after PI3K inhibition as compared to vehicle-treated mice, indicating that the spikes in insulin could be causing transient increases in glucose uptake in these tumours (Fig. 1d).

To test whether these spikes in insulin were stimulating PI3K signalling in the context of PI3K inhibition, we treated KPC cells in vitro with PI3K inhibitors in the presence or absence of 10 ng ml⁻¹ insulin (the amount observed in the mice within 15–30 min of drug administration; Fig. 1d). This level of insulin was sufficient to partially rescue PI3K signalling in the continued presence of PI3K inhibitors, as indicated by partial re-activation of phosphorylated AKT (pAKT) and almost complete reactivation of phosphorylated S6 (pS6), a reporter of growth signalling through the mTORC1 complex (Fig. 2a, Supplementary Fig. 1). In addition, this enhanced signalling correlated with a partial recovery of cellular proliferation (Fig. 2b, c). Insulin also stimulated proliferation in the presence of a PI3K inhibitor in a variety of other tumour cell lines and patient-derived organoids¹⁶ (Extended Data Fig. 2a–g). The amount of stimulation was not uniform across all cell lines, as would be expected in tumours with variable expression of the insulin receptor and differential dependence on PI3K signalling for growth. These observations support the conclusions that insulin is a potent activator of PI3K signalling in certain tumours, and that elevation of serum insulin following administration of a PI3K inhibitor can reactivate PI3K signalling and potentially other PI3K-independent responses to insulin in both normal tissues and tumours.

Research into diabetes and treatment of patients with diabetes have resulted in the development of numerous approaches to manage blood glucose and insulin levels. Using these tools, we sought to identify ways to augment PI3K inhibitor therapies by circumventing the acute glucose-insulin feedback. We chose to evaluate metformin and inhibitors of sodium-glucose co-transporter 2 (SGLT2), both of which are

¹Meyer Cancer Center, Weill Cornell Medicine, New York, NY, USA. ²Institute of Pathology and Molecular Pathology, University Hospital Zurich, Zurich, Switzerland. ³Englander Institute for Precision Medicine, Weill Cornell Medicine-New York Presbyterian Hospital, New York, NY, USA. ⁴Department of Medicine, Division of Hematology and Oncology, Columbia University Medical Center and New York Presbyterian Hospital, New York, NY, USA. ⁵Weill Cornell Medicine/Rockefeller University/Sloan Kettering Tri-Institutional MD-PhD Program, New York, NY, USA. ⁶Weill Cornell Graduate School of Medical Sciences, New York, NY, USA. ⁷Division of Endocrinology, Department of Medicine, Weill Cornell Medicine, New York, NY, USA. ⁸Institute for Computational Biomedicine, Weill Cornell Medicine, New York, NY, USA. ⁹Department of Pathology, Weill Cornell Medicine, New York, NY, USA. ¹⁰Department of Medicine, Division of Hematology and Medical Oncology, Weill Cornell Medicine, New York, NY, USA. ¹¹Department of Biomedical Research and the Center for Precision Medicine, University of Bern and the Inselspital, Bern, Switzerland.
*e-mail: sm3252@cumc.columbia.edu; lcantley@med.cornell.edu

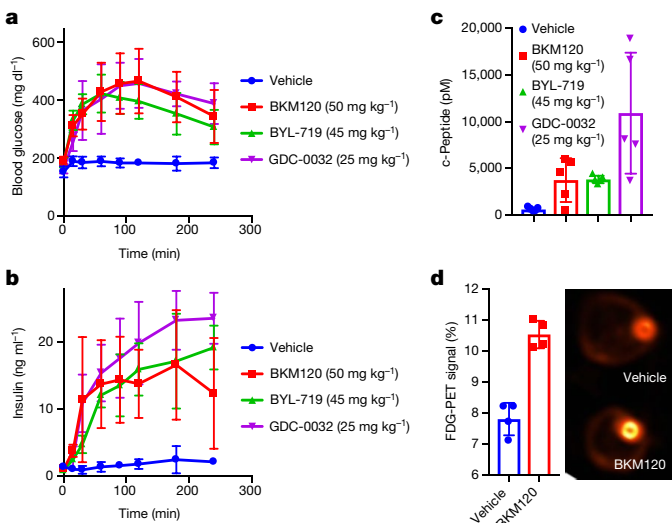


Fig. 1 | Treatment with PI3K inhibitors causes systemic feedback that results in increases in blood glucose and insulin. **a, b,** Mean (\pm s.d.) blood glucose (**a**) and insulin (**b**) levels in mice treated with the indicated PI3K inhibitor compounds ($n = 5$ per arm, $P < 0.0001$ by two-way ANOVA for all curves as compared to vehicle). **c,** Mean (\pm s.d.) of c-peptide levels assessed at 240 min (P values comparing vehicle to BKM120, BYL-719, and GDC-0032 by two-sided t -test were 0.017, <0.0001 and 0.007 respectively). **d,** Mean per cent (\pm s.d.) of FDG-PET signal (left) of orthotopically implanted KPC tumours imaged (right) 90 min after a single treatment with BKM120 ($n = 4$ per arm, $P = 0.0002$, by two-sided t -test).

extensively used to treat diabetes^{17–20}, as well as a ketogenic diet in our mouse models of cancer. Metformin was chosen because it has an extremely low toxicity profile and is commonly used in patients with diabetes or pre-diabetes to increase their insulin sensitivity, which reduces hyperglycaemia and insulin levels²⁰. Metformin is also commonly used in trials of PI3K inhibitors to manage patients who become chronically hyperglycaemic^{21–23}. SGLT2 inhibitors are also generally well tolerated and work by inhibiting the glucose transporters that are responsible for the reabsorption of glucose in the kidney. The rationale for using a ketogenic diet was to deplete hepatic glycogen stores and thereby limit the acute release of glucose from the liver that occurs following PI3K inhibition. Ketogenic diets have been used to treat patients with epilepsy since the 1970s and have been shown to reduce blood glucose levels and increase insulin sensitivity as compared to normal western diets^{7,24}.

To test whether these approaches could limit acute glucose–insulin feedback and alter signalling in tumours, treatment-naïve mice bearing KPC tumour allografts were placed on a ketogenic diet or treated with metformin for 10 days before a single treatment with the PI3K inhibitor BKM120. During this treatment, blood glucose was monitored and, after 3 h, c-peptide (a surrogate for blood insulin) was measured (Fig. 3a, b). In some mice, tumours were removed after 90 min and stained for pS6, a reporter of mTORC1 activity (Fig. 3c, d). These results demonstrated that pretreatment with metformin had only a minimal effect on the PI3K inhibitor-induced elevation in blood glucose and insulin levels or on growth signalling through mTORC1. By contrast, both the SGLT2 inhibitor and the ketogenic diet decreased hyperglycaemia and reduced the release of insulin in response to BKM120 treatment, and these effects correlated with reduced signalling through mTORC1 in the tumour. Similar effects were seen in mice treated with the p110 α -specific inhibitor BYL-719, in which the response of KPC allografts to BYL-719 was enhanced in a manner concordant with the relative ability of each treatment to reduce serum insulin levels (Fig. 3e–g, Extended Data Fig. 3a–d).

Various hormones and metabolites can reactivate growth in the setting of PI3K inhibition. To test whether the enhancement in tumour

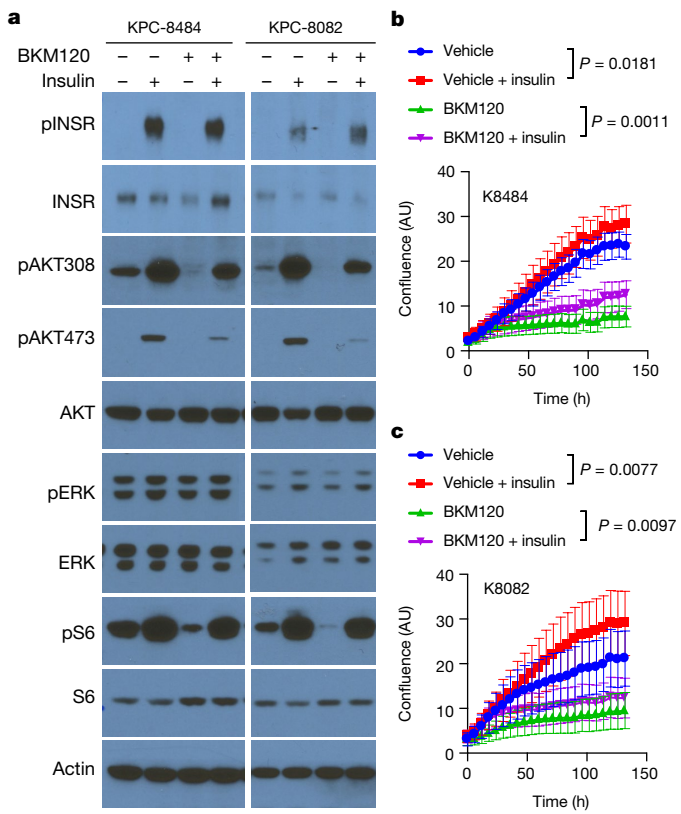


Fig. 2 | Effect of feedback levels of insulin on cellular proliferation, signalling and survival. **a,** Western blot analysis of KPC cell lines K8484 and K8082 treated with or without PI3K inhibitor BKM120 (1 μ M) in the presence or absence of physiological feedback levels of insulin (10 ng mL⁻¹). Similar results were observed in three independent experiments. **b, c,** Mean (\pm s.d.) confluence of KPC cell lines K8484 and K8082 over time grown in the presence or absence of insulin (10 ng mL⁻¹) and BKM120 (1 μ M). P values determined by ANOVA comparing conditions with or without insulin are shown; $n = 16$ biologically independent samples per group. AU, arbitrary units.

signalling and growth was mediated directly by insulin, we generated a doxycycline-inducible short hairpin RNA (shRNA) to target the insulin receptor in KPC tumours (Extended Data Fig. 4a, Supplementary Fig. 2). Induction of this hairpin in the absence of a PI3K inhibitor had little effect on tumour growth. However, induction of the hairpin at the initiation of BYL719 treatment resulted in tumour shrinkage and was almost as effective as the ketogenic diet (Fig. 4a). This result supports a model in which the insulin receptor does not have a major role in tumour growth until supra-physiological amounts of insulin are released following treatment with a PI3K inhibitor. The specificity of this effect was further corroborated by combining the PI3K inhibitor BKM120 with OSI-906, which inhibits the insulin receptor and the IGF1 receptor. This had a great effect on the growth of KPC allografts than either drug alone (Extended Data Fig. 4b–g). Notably, feeding a ketogenic diet to mice bearing tumours with insulin receptor knock-down (Fig. 4a) or to mice treated with OSI-906 (Extended Data Fig. 4b) in the absence of a PI3K inhibitor provided little or no enhancement of therapeutic response.

To further test whether the improved response to PI3K inhibitors while on a ketogenic diet is a consequence of lowering blood insulin levels, we attempted to ‘rescue’ the PI3K reactivation using exogenous insulin. A cohort of mice bearing *Pik3ca* mutant breast tumour allografts were treated with a combination of a ketogenic diet and BYL-719, and then given 0.4 mU of insulin 15 min after each dose of PI3K inhibitor (Fig. 4b). The addition of insulin markedly reduced the therapeutic benefit of supplementing PI3K inhibitor therapy with a ketogenic diet, and also rescued tumour growth in allografted KPC tumours (Extended

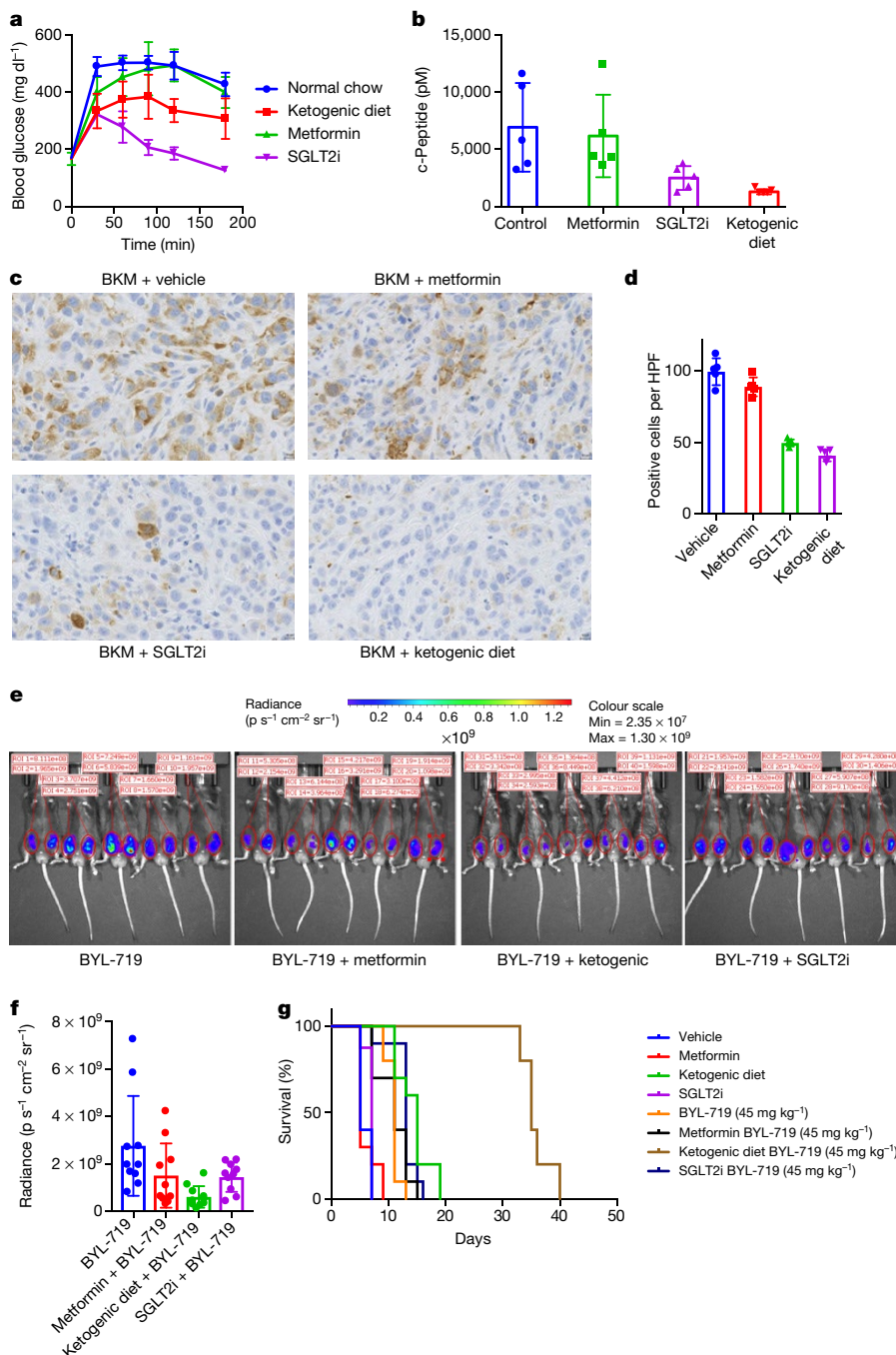


Fig. 3 | Targeting PI3K-inhibitor-induced glucose/insulin feedback in vivo. **a**, Mean (\pm s.d.) blood glucose levels over time of wild-type c57/bl6 mice bearing syngeneic K8484 KPC allografted tumours and pretreated with metformin, SGLT2-inhibitor (SGLT2i), or a ketogenic diet, after treatment with a single dose of BKM120 ($n = 5$ mice). P values calculated by two-way repeated measures ANOVA for metformin, SGLT2i, and the ketogenic diet were 0.2136 (not significant), <0.0001 , and 0.007, respectively. **b**, Mean (\pm s.d.) blood levels of c-peptide of the same mice ($n = 5$) taken 180 min after treatment with BKM120. P values calculated by unpaired two-sided t -test for metformin, SGLT2i, and ketogenic diet were 0.7566 (not significant), 0.0386, and 0.0117, respectively. **c**, Immunohistochemical staining for pS6 (ser-235) to observe the level

of active PI3K signalling in these tumours. **d**, Quantification of staining shown as mean (\pm s.d.) number of positive cells per high power field (HPF) ($n = 5$ mice per group). P values comparing pS6-positive cells in tumours treated with BKM120 alone compared to those treated with BKM120 in combination with metformin, SGLT2i, or the ketogenic diet using two-sided t -tests were 0.6186, <0.0001 and <0.0001 , respectively. **e**, IVIS images of luciferase reporter luminescence in mice with KPC K8484 tumours after 12 days of treatment with the PI3K α -specific inhibitor BYL-719 alone or in combination with metformin, ketogenic diet, or SGLT2i ($n = 10$ tumours per arm). **f**, Mean (\pm s.d.) luminescence from images of these tumours. **g**, Survival analysis of these mice. $P = 0.0019$ and 0.0001 , respectively, as determined by log-rank (Mantel–Cox) test.

Data Fig. 4h). It should be noted that the combination of the ketogenic diet, insulin, and BYL-719 was not well-tolerated in young mice, so ethical endpoints were reached in this cohort. Together these data strongly support a model in which a ketogenic diet improves responses to PI3K inhibitors by reducing blood insulin and the consequent ability of insulin to activate the insulin receptor in tumours.

In this study, we evaluated the ability of a ketogenic diet to improve responses to PI3K inhibitors in tumours with a wide range of genetic aberrations. Therapeutic benefit was observed in patient-derived xenograft models of advanced endometrial adenocarcinoma (harbouring a PTEN deletion and PIK3CA mutation) and bladder cancer (FGFR-amplified) as well as in syngeneic allograft models of *Pik3ca* mutant

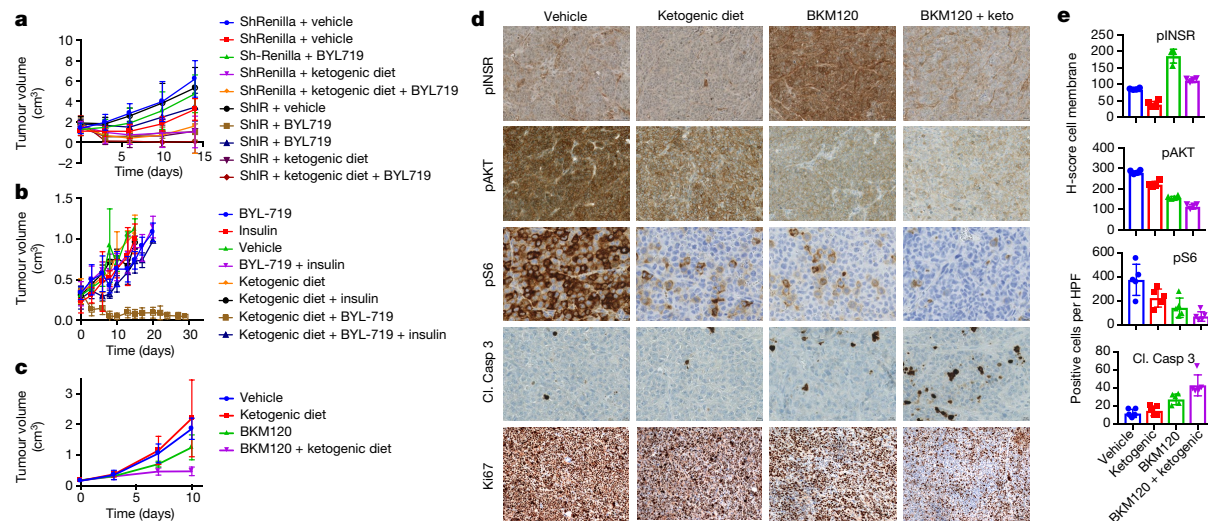


Fig. 4 | Effect of circumventing the on target glucose–insulin feedback of PI3K inhibitors upon tumour growth. **a**, Graph of mean (\pm s.d.) tumour volumes of K8484 KPC with doxycycline-inducible shRNA targeting Renilla (shRenilla) or insulin receptor (shIR), treated with doxycycline and as indicated with the PI3K inhibitor BYL-719 and/or co-administration of a ketogenic diet ($n = 8, 9, 8, 10$, for shRenilla tumours treated with vehicle, BYL719, ketogenic diet, and BYL + ketogenic diet, respectively, and $n = 8, 8, 10, 8$ for shIR tumours treated with vehicle, BYL719, ketogenic diet, and BYL + ketogenic diet, respectively). **b**, Mean (\pm s.d.) volumes of ES272 Pik3ca mutant breast cancer allograft tumours treated with BYL-719 and/or insulin along with the ketogenic diet (keto) as indicated. $n = 3, 3, 5, 5, 5, 3, 4, 4$ for vehicle, insulin, BYL, BYL + insulin, ketogenic diet, ketogenic + insulin, ketogenic + BYL, and

breast cancer and *MLL-AF9* driven acute myeloid leukaemia (AML) (Fig. 4c, Extended Data Figs. 5–7).

The addition of the ketogenic diet improved drug efficacy with an array of agents that target the PI3K pathway in addition to BKM120 and BYL719, including the pan-PI3K inhibitor GDC-0941, the PI3K- β -sparing compound GDC-0032, the mTOR/PI3K dual inhibitor GDC-0980, and the recently approved PI3K- α/δ inhibitor Copanlisib (Extended Data Fig. 5). It is important to note that treatment with the ketogenic diet alone had variable effects in different tumour models, indicating that the dietary changes themselves were insufficient to cause the tumour responses observed across the mouse models. In some instances, such as the AML model, the ketogenic diet alone accelerated disease progression, suggesting that this diet may be detrimental for some patients with cancer when used in isolation.

Our data suggest that insulin feedback limits the efficacy of PI3K inhibition in several tumour models. By reducing the systemic insulin response, the addition of a ketogenic diet to BKM120 reduced immunohistochemical markers of insulin signalling in *PTEN/PIK3CA* mutant endometrial patient-derived xenograft (PDX) tumours, compared to tumours from mice treated with BKM120 alone. In these tumours, the ketogenic diet enhanced the ability of BKM120 to reduce levels of phosphorylated insulin receptor, phosphorylated AKT and phosphorylated S6 and this reduction in signalling correlated with decreased levels of proliferation as shown by Ki67 staining, and increased levels of apoptosis as indicated by cleaved caspase 3 staining (Fig. 4d, e).

While these data do not exclude insulin-independent effects of combining PI3K inhibition with anti-glycaemic therapy, they demonstrate that using this approach has the potential to substantially increase the therapeutic efficacy of these compounds. In light of these results, it may also be important to think about how common clinical practices such as intravenous glucose administration, glucocorticoid use, or providing patients with glucose-laden nutritional supplements may impact therapeutic responses. As therapeutic agents that target this critical oncogenic pathway are brought through clinical trials, they should be

ketogenic + BYL + insulin, respectively. **c**, Mean (\pm s.d.) tumour volume of endometrial PDXs treated with BKM120 and/or a ketogenic diet ($n = 5$ per arm, $P = 0.0028$ by ANOVA comparison between BKM120 alone and BKM120 + ketogenic diet). **d, e**, Histology and quantification of phospho-insulin receptor (pINSR), pAKT, pS6, cleaved caspase 3 (Cl. Casp 3), and Ki67 of the tumours from **d** taken 4 h after the last treatment with vehicle, ketogenic diet, BKM120, or the combination of the ketogenic diet with BKM120 (BKM120 + keto). Quantification is depicted as score per HPF, four images were taken for each of the $n = 5$ mice. P values from two-sided *t*-tests comparing the blinded scoring in BKM120-treated tumours with those treated with BKM120 + ketogenic diet were 0.005, 0.005, 0.017 and 0.028 for pINSR, pAKT, pS6 and Cl. Casp 3, respectively. H-score denotes intensity and percent of cells with staining at the cell membrane.

paired with strategies such as SGLT2 inhibition or the ketogenic diet to limit this self-defeating systemic feedback.

Online content

Any Methods, including any statements of data availability and Nature Research reporting summaries, along with any additional references and Source Data files, are available in the online version of the paper at <https://doi.org/10.1038/s41586-018-0343-4>

Received: 25 July 2017; Accepted: 26 June 2018;

Published online 4 July 2018.

- Kandoth, C. et al. Mutational landscape and significance across 12 major cancer types. *Nature* **502**, 333–339 (2013).
- Millis, S. Z., Ikeda, S., Reddy, S., Gatalica, Z. & Kurzrock, R. Landscape of phosphatidylinositol-3-kinase pathway alterations across 19784 diverse solid tumors. *JAMA Oncol.* **2**, 1565–1573 (2016).
- Bendell, J. C. et al. Phase I, dose-escalation study of BKM120, an oral pan-class I PI3K inhibitor, in patients with advanced solid tumors. *J. Clin. Oncol.* **30**, 282–290 (2012).
- Juric, D. et al. Phase I dose-escalation study of taselisib, an oral PI3K inhibitor, in patients with advanced solid tumors. *Cancer Discov.* **7**, 704–715 (2017).
- Patnaik, A. et al. First-in-human phase I study of copanlisib (BAY 80-6946), an intravenous pan-class I phosphatidylinositol 3-kinase inhibitor, in patients with advanced solid tumors and non-Hodgkin's lymphomas. *Ann. Oncol.* **27**, 1928–1940 (2016).
- Mayer, I. A. et al. A Phase Ib study of alpelisib (BYL719), a PI3K α -specific inhibitor, with letrozole in ER $^{+}$ /HER2 $^{-}$ metastatic breast cancer. *Clin. Cancer Res.* **23**, 26–34 (2017).
- Hopkins, B. D., Goncalves, M. D. & Cantley, L. C. Obesity and cancer mechanisms: cancer metabolism. *J. Clin. Oncol.* **34**, 4277–4283 (2016).
- Fruman, D. A. et al. The PI3K pathway in human disease. *Cell* **170**, 605–635 (2017).
- Belardi, V., Gallagher, E. J., Novosyadlyy, R. & LeRoith, D. Insulin and IGFs in obesity-related breast cancer. *J. Mammary Gland Biol. Neoplasia* **18**, 277–289 (2013).
- Gallagher, E. J. & LeRoith, D. Minireview: IGF, insulin, and cancer. *Endocrinology* **152**, 2546–2551 (2011).
- Kiln-Drori, A. J., Azoulay, L. & Pollak, M. N. Cancer, obesity, diabetes, and antidiabetic drugs: is the fog clearing? *Nat. Rev. Clin. Oncol.* **14**, 85–99 (2017).

12. Ma, J. et al. A prospective study of plasma c-peptide and colorectal cancer risk in men. *J. Natl. Cancer Inst.* **96**, 546–553 (2004).
13. Xu, J. et al. Association between markers of glucose metabolism and risk of colorectal cancer. *BMJ Open* **6**, e011430 (2016).
14. Ma, J. et al. Prediagnostic body-mass index, plasma c-peptide concentration, and prostate cancer-specific mortality in men with prostate cancer: a long-term survival analysis. *Lancet Oncol.* **9**, 1039–1047 (2008).
15. Olive, K. P. et al. Inhibition of Hedgehog signaling enhances delivery of chemotherapy in a mouse model of pancreatic cancer. *Science* **324**, 1457–1461 (2009).
16. Pauli, C. et al. Personalized in vitro and in vivo cancer models to guide precision medicine. *Cancer Discov.* **7**, 462–477 (2017).
17. Komoroski, B. et al. Dapagliflozin, a novel, selective SGLT2 inhibitor, improved glycemic control over 2 weeks in patients with type 2 diabetes mellitus. *Clin. Pharmacol. Ther.* **85**, 513–519 (2009).
18. Demin, O., Jr, Yakovleva, T., Kolobkov, D. & Demin, O. Analysis of the efficacy of SGLT2 inhibitors using semi-mechanistic model. *Front. Pharmacol.* **5**, 218 (2014).
19. Pollak, M. Metformin and other biguanides in oncology: advancing the research agenda. *Cancer Prev. Res. (Phila.)* **3**, 1060–1065 (2010).
20. Pollak, M. Potential applications for biguanides in oncology. *J. Clin. Invest.* **123**, 3693–3700 (2013).
21. Saura, C. et al. Phase I b study of buparlisib plus trastuzumab in patients with HER2-positive advanced or metastatic breast cancer that has progressed on trastuzumab-based therapy. *Clin. Cancer Res.* **20**, 1935–1945 (2014).
22. Juvekar, A. et al. Combining a PI3K inhibitor with a PARP inhibitor provides an effective therapy for BRCA1-related breast 1158/2159–8290.CD-11–0336
23. Puchalska, P. & Crawford, P. A. Multi-dimensional roles of ketone bodies in fuel metabolism, signaling, and therapeutics. *Cell Metab.* **25**, 262–284 (2017).
24. Sampaio, L. P. Ketogenic diet for epilepsy treatment. *Arq. Neuropsiquiatr.* **74**, 842–848 (2016).

Acknowledgements This work was supported by NIH grant R35 CA197588 (L.C.C.), R01 GM041890 (L.C.C.), U54 U54CA210184 (L.C.C.), Breast Cancer Research Foundation (L.C.C.) and the Jon and Mindy Gray Foundation (L.C.C.). The content is solely the responsibility of the authors and does not necessarily

represent the official views of the National Institutes of Health. We appreciate the help of the small animal imaging core at MSKCC for assistance with FDG-PET imaging and the Columbia Irving Cancer Center Flow Core Facility, funded in part through Center Grant P30CA013696.

Reviewer information *Nature* thanks V. Longo, M. Pollak, C. Rask-Madsen and the other anonymous reviewer(s) for their contribution to the peer review of this work.

Author contributions B.D.H., S.M. and L.C.C. conceived of the project. B.D.H., C.P., X.D., Y.M. and D.W. performed the mouse experiments. S.C.A., C.P., B.D.H., E.M.H. and X.L. did the culture assays. S.C.A. performed immunoblotting. B.D.H., C.H. and M.D.G. assessed the impact of treatments on cellular and systemic metabolism. D.G.W. and S.C.A. cloned and validated the IR knockdowns. M.R.L. and R.B. performed the data analysis. C.P., A.S., H.B., M.A.R., L.C.C., S.M., B.D.H. and R.B. assisted with implementation of patient-derived models. All authors assisted with data interpretation and contributed to the writing and editing of the manuscript.

Competing interests L.C.C. is a founder and member of the board of directors of Agios Pharmaceuticals and is a founder and receives research support from Petra Pharmaceuticals. S.M. is a founder and on the board of Vor Pharmaceuticals. These companies are developing novel therapies for cancer. All other authors declare no competing interests.

Additional information

Extended data is available for this paper at <https://doi.org/10.1038/s41586-018-0343-4>.

Supplementary information is available for this paper at <https://doi.org/10.1038/s41586-018-0343-4>.

Reprints and permissions information is available at <http://www.nature.com/reprints>.

Correspondence and requests for materials should be addressed to S.M. or L.C.C.

Publisher's note: Springer Nature remains neutral with regard to jurisdictional claims in published maps and institutional affiliations.

METHODS

Mice procurement and treatment. All animal studies were conducted following IACUC approved animal protocols (#2013-0116) at Weill Cornell Medicine and (AC-AAQ5405) at Columbia University. Ethical requirements for the treatment of animals were followed for all of the animal studies as per institutional guidelines. Mice were maintained in temperature- and humidity-controlled specific pathogen-free conditions on a 12-h light/dark cycle and received a normal chow diet (PicoLab Rodent 20 5053 laboratory Diet St. Louis, MO) or ketogenic diet (Thermo-Fisher AIN-76A) with free access to drinking water. Diets were composed as indicated in Supplementary Table 1. Owing to the nature of the diets used, blinding was not possible. No statistical methods were used to predetermine sample size.

For solid tumour studies Nude (genotype) and C57/BL6 mice were purchased at 8 weeks of age from Jackson laboratories (Bar Harbour, ME). They were injected with $0.5\text{--}1 \times 10^6$ cells in a 1:1 mix of growth media and matrigel (Trevigen, # 3433-005-R1) and tumours were allowed to grow to a minimum diameter of 0.6cm before the initiation of treatment. Tumours that did not meet this criterion at the time of treatment initiation were not used for experimentation.

For AML studies 10-12 weeks old male C57BL/6J mice were used for MLL-AF9 Ds-Red AML study (Approved protocol AC-AAQ5405). For pre-treatment study with MLL-AF9 Ds-Red cells, keto and Keto/BKM group mice were given a ketogenic diet for 10 days before injection with MLL-AF9 Ds-Red cells (2×10^5 per mouse in 200 μl) via lateral tail vein. The day after iv injection, the mice were given 0.5% carboxymethyl cellulose (CMC) as vehicle control or BKM120 (37.5 mg/kg) by oral gavage for two weeks (5 out of 7 days). The mice were euthanized after two-week treatment to check the bone marrow for AML progress. The mice were euthanized and one femur and tibia were removed from each mouse. The bone marrow cells were flushed with PBS (2% FBS). The red blood cells were lysed with ACK lysis buffer (Invitrogen). DAPI was used to exclude dead cells. The DS-red AML cells from the BM were analysed with BD LSRII. The tumour progress was also monitored via IVIS spectrum machine. For co-current treatment study with MLL-AF9 Ds-Red cells, the mice were injected with MLL-AF9 Ds-Red cells (2×10^5 per mouse in 200 μl) via lateral tail vein. The day after iv injection, the mice were given vehicle or BKM120 (37.5 mg/kg) by oral gavage for two weeks. The Keto or Keto/BKM group were changed to a ketogenic diet on the same day. The mice were euthanized after two-week treatment to check the bone marrow for AML progress.

To check whether Keto/BKM treatment affects the AML engraftment, Keto and Keto/BKM group mice were given a ketogenic diet for 10 days, then treated with vehicle or BKM120 by oral gavage for two weeks. The mice were then injected with MLL-AF9 Ds-Red cells (2×10^5 per mouse in 200 μl) via lateral tail vein. Two weeks after the iv injection, the mice were euthanized to check the bone marrow for AML burden.

The survival study, pre-treatment study, and co-current treatment were conducted at the same time. The mice were treated with vehicle or BKM120 (5 out of 7 days) until spontaneous death, or mice were euthanized when they appeared to be very sick (reduced spontaneous activity, unkempt coat, and dehydrated appearance), achieved body weight loss over 20%, or demonstrated signs of limb paralysis. **Compounds.** GDC-0032, MK2206, BEZ235, BKM-120, GDC-0941, GDC-0980, and Canagliflozin were all procured from Medchem Express (Monmouth Junction, NJ) and given via oral gavage in 100 μl . Metformin was procured from Sigma Aldrich (St. Louis, MO). BAY-80 6946 and OSI-906 came from Selleckchem catalogue #S2802 and #S1091 respectively. The targeting information for these compounds is displayed in Supplementary Table 3. IC₅₀ data was obtained from the Selleckchem website (Selleckchem.com). The canagliflozin was administered 60 min before the PI3K pathway inhibitors so that its optimal efficacy lined up with the peak glucose levels. Mice treated with metformin were pretreated for 10 days before BKM120 treatment. Ketogenic diet was initiated at the time of initial PI3K inhibitor treatment unless otherwise stated. Doxycycline was procured from Sigma (St. Louis, Missouri) catalogue number D3072-1ML and administered via intraperitoneal injection once daily at a dose of 3mg/kg.

Culture. Murine pancreas cell lines were a gift from K. Olive, Columbia University¹⁵. Murine breast lines were a gift from R. Parsons, Mount Sinai School of Medicine. PDX models were derived by the Englehardt Institute of Precision Medicine in accordance with an IRB approved protocol as described^{16,25}. Cell lines HEK293, HCC-38, MDA-MB-468, PC-3, BT-549 were purchased from ATCC and grown in DMEM supplemented with 10% FBS and 1% Pen/Strep. HCT-116 and DLD-1 isogenic lines with and without PTEN deletion were kindly provided by the Laboratory of Todd Waldman²⁶. A chart of cells/organoids is in Supplementary Table 2, with known oncogenic alterations as described in publications cited above or as available from the ATCC (https://www.atcc.org/~media/PDFs/Culture%20Guides/Cell_Lines_by_Gene_Mutation.ashx). Authentication was not required for the cells that came directly from ATCC. Key genetic alterations of mouse lines

were confirmed via genotyping for transgenes. Mutant HCT-116 and DLD-1 lines from the Waldman lab were validated by western blot analysis to demonstrate PTEN deletion.

For signalling assays, cells were washed 1x in PBS and placed in starvation media (-FBS) for 6–18 h depending upon cell line, and treated 1 h before harvesting with PI3K inhibitors as indicated alone or in combination with insulin 10 min before harvesting. Three dimensional culture and dose response experiments of patient derived organoids were run as previously described¹⁶. In brief, ~1,000 cells were plated in 10 μl of 1:1 matrigel to culture media in 96 well angiogenesis plates and allowed to solidify for 30 min at 37 degrees before 70 μl of culture media was added. Organoids were then treated in triplicate in a log scale dose response and CellTiter-Glo assay (Promega) was run at 96 h to determine the IC₅₀ values.

Knockdown of insulin receptor was achieved using a doxycycline-inducible shRNA strategy. For generation of miR-E shRNAs, 97-mer oligonucleotides were purchased (IDT Ultramers) coding for predicted shRNAs using an siRNA prediction tool Splash RNA, <http://splashrna.mskcc.org>²⁷. Oligonucleotides were PCR amplified using the primers miRE-Xho-fw (5'-TGAACCTGAGAAAGGTATATTGCTGTTGACAGTGAGCG-3') and miRE-Eco-rev (5'-TGAACCTGAGAAAGGTATATTGCTGTTGACAGTGAGCG-3'). PCR products were purified and both PCR product and LT3GEPIR²⁸ vectors were double digested with EcoRI-HF and XhoHI. PCR product and vector backbone were ligated and transformed in Stbl3 competent cells and grown at 32 °C overnight. Colonies were screened using the primer miRE-fwd (5'-TGTTTGAATGAGGCTTCAGTAC-3'). Renilla, TGCTGTTGACAGTGAGC-GCAGGAATTATAATGCTTATCTATAGTAAGGCCACAGAT

GTATAGATAAGCATTATAATCCTATGCCTACTGCCTCGGA; INSR4, TGCTGTTGACAGTGAGCGGGGTTCATGCTGTTCAATAGTGAAG CCACAGATGTATTGAGAACAGCATGAACCCATGCCTACTGCCTCGGA. **Immunoblotting.** Cell lysates were prepared in 1x CST Cell Lysis Buffer #9803, (Danvers MA). Total protein concentration was evaluated with the BCA kit (Pierce) 23227. The lysates were run out on 4–20% Tris-Glycine Gels (ThermoFisher, Carlsbad CA). Primary antibodies against pAKT473, pAKT308, pS6, pTYR, AKT, and S6 were procured from Cell Signaling (Danvers, MA), and were used overnight at 1:1,000 in 5% bovine serum albumin. Actin and tubulin antibodies came from Sigma Aldrich and were used at 1:5,000 in 5% milk. All these antibodies were visualized with HRP conjugated secondary antibodies from Jackson Immuno at 1:5,000 in 5% milk.

Immunohistochemistry. Tumour sections (3 μm) were antigen retrieved with 10 mmol/L citrate acid, 0.05% Tween 20, pH6.0, and incubated with antibodies as indicated (Ki67 (Abcam, ab16667) 1:500; cleaved caspase-3 (Asp175; 5A1E; Cell Signaling Technology, 9664) 1:200; phospho-INSR (Tyr 1162; Thermo Fisher #AHR0271) 1:100; phospho-AKT (Ser473; Cell Signaling Technology, 8101) 1:20; and phospho-S6 ribosomal protein (Ser235/236; Cell Signaling Technology, 2211) 1:300).

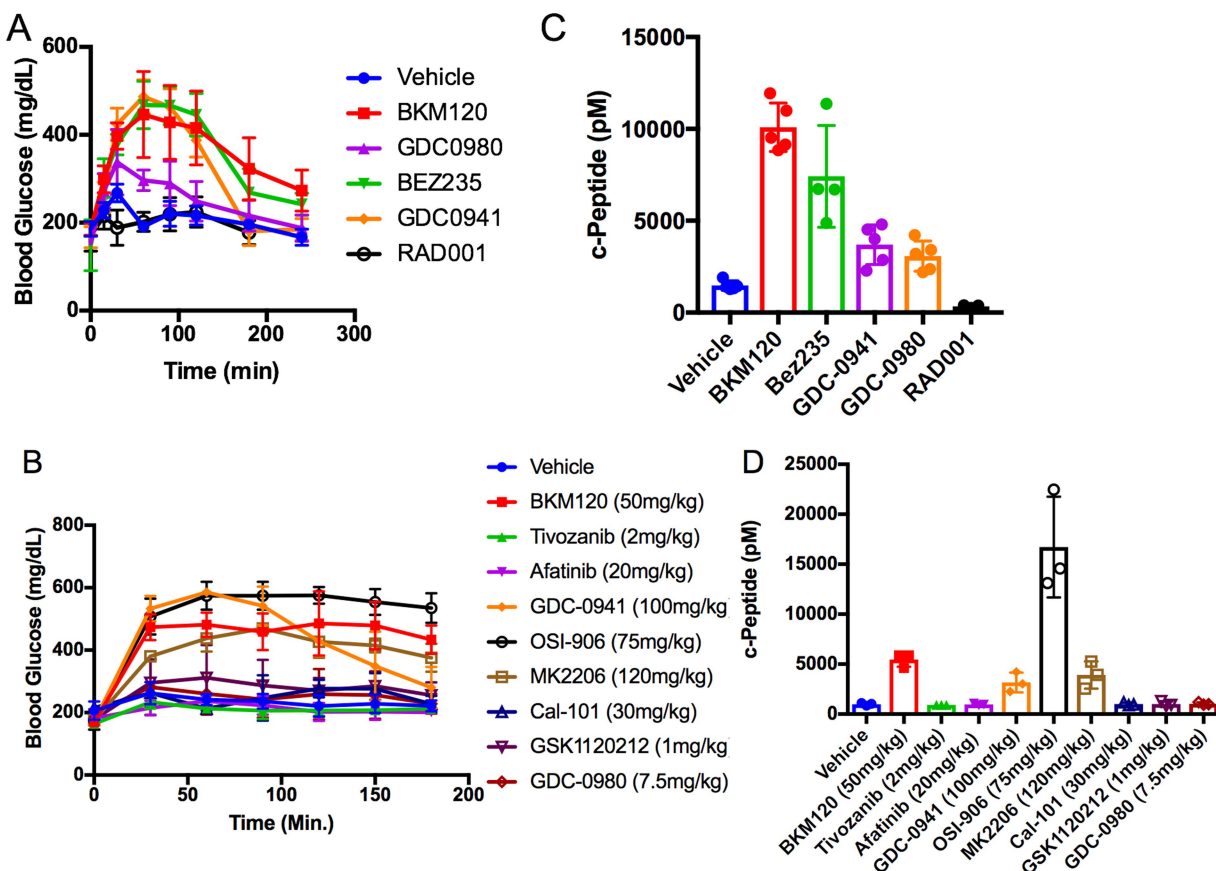
Blood measurements. For assessment of blood glucose, 10 μl of blood was taken from the tail of mice before treatment (time 0) and then again at the indicated time points (15, 30, 60, 90, 120, 180 min) using a OneTouch Ultra Glucometer. At end point >100 μl of blood was drawn from the mice into EDTA tubes (Sarstedt #16.444). Blood was centrifuged (10,000g for 10 min at 4 °C), and plasma was stored at –20 °C. Plasma β -hydroxybutyrate, triglyceride (Stambio Laboratory, Boerne, TX), serum insulin, and c-peptide (APLCO Diagnostics, Salem, NH) levels were quantified by ELISA.

FDG-PET. Male c57/bl6 mice ($n = 4/\text{arm}$) bearing orthotopic pancreatic adenocarcinoma allografts were injected with 200–250 μCi [⁸⁹Zr]liposomes (3–4 μmol lipid) in 200–250 μL PBS solution into the tail vein. At the time of peak blood insulin feedback 90 min post BKM120 injection animals were anaesthetized and scans were then performed using an Inveon PET/CT scanner (Siemens Healthcare Global). Whole body PET scans were performed recording a minimum of 50 million coincident events, with a duration of 10 min. The energy and coincidence timing windows were 350–750 keV and 6 ns. The data were normalized to correct for non-uniformity of response of the PET, dead-time count losses, positron branching ratio, and physical decay to the time of injection. The counting rates in the reconstructed images were converted to activity concentrations (percentage injected dose [%ID] per gram of tissue) by use of a system calibration factor derived from the imaging of a phantom containing ⁸⁹Zr. Images were analysed using ASIPro VMTM software (Concorde Micro-systems). Quantification of activity concentration was done by averaging the maximum values in at least 5 ROIs drawn on adjacent slices of the pancreatic tumours.

Reporting summary. Further information on experimental design is available in the Nature Research Reporting Summary linked to this paper.

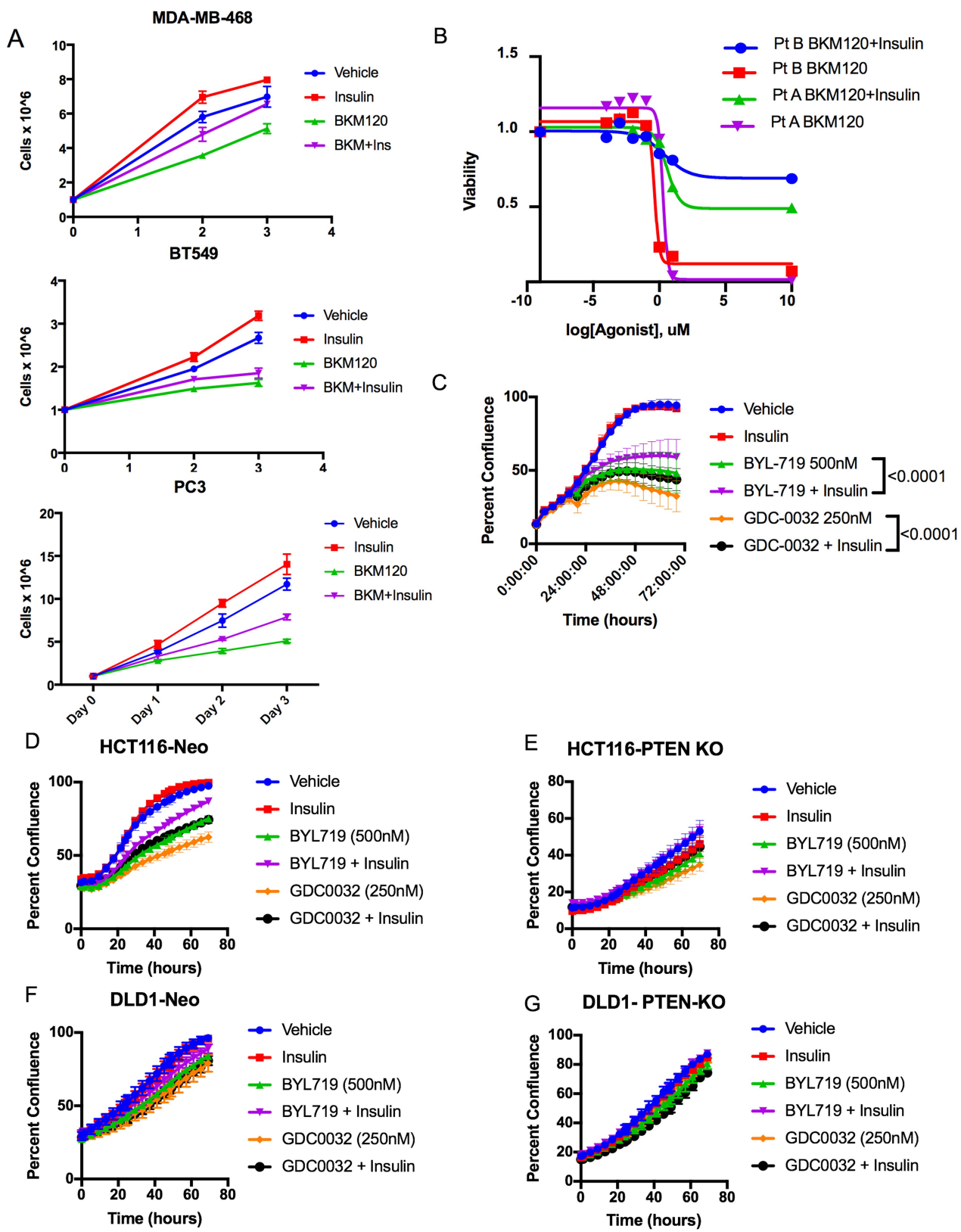
Data availability. Source data for Figs. 1, 3 and 4 and Extended Data Figs. 1, 3–7 are provided in the online version of the paper. All other data are available from the corresponding author upon reasonable request.

25. Pauli, C. et al. An emerging role for cytopathology in precision oncology. *Cancer Cytopathol.* **124**, 167–173 (2016).
26. Lee, C., Kim, J. S. & Waldman, T. PTEN gene targeting reveals a radiation-induced size checkpoint in human cancer cells. *Cancer Res.* **64**, 6906–6914 (2004).
27. Pelosof, R. et al. Prediction of potent shRNAs with a sequential classification algorithm. *Nat. Biotechnol.* **35**, 350–353 (2017).
28. Fellmann, C. et al. An optimized microRNA backbone for effective single-copy RNAi. *Cell Reports* **5**, 1704–1713 (2013).
29. Douris, N. et al. Adaptive changes in amino acid metabolism permit normal longevity in mice consuming a low-carbohydrate ketogenic diet. *Biochim. Biophys. Acta* **1852**, 2056–2065 (2015).



Extended Data Fig. 1 | Blood glucose and c-peptide levels after treatment with agents that target the PI3K pathway. a, b, Mean \pm s.d. blood glucose levels over time where time 0 is the time of treatment with the indicated inhibitor. $n=5$ and 3 mice per arm for **a** and **b**, respectively. **c, d,** Mean \pm s.d. c-peptide levels from mice in **a** and **b** taken 240 and 180 min after treatment with indicated inhibitors. **c**, $n=5$ for vehicle,

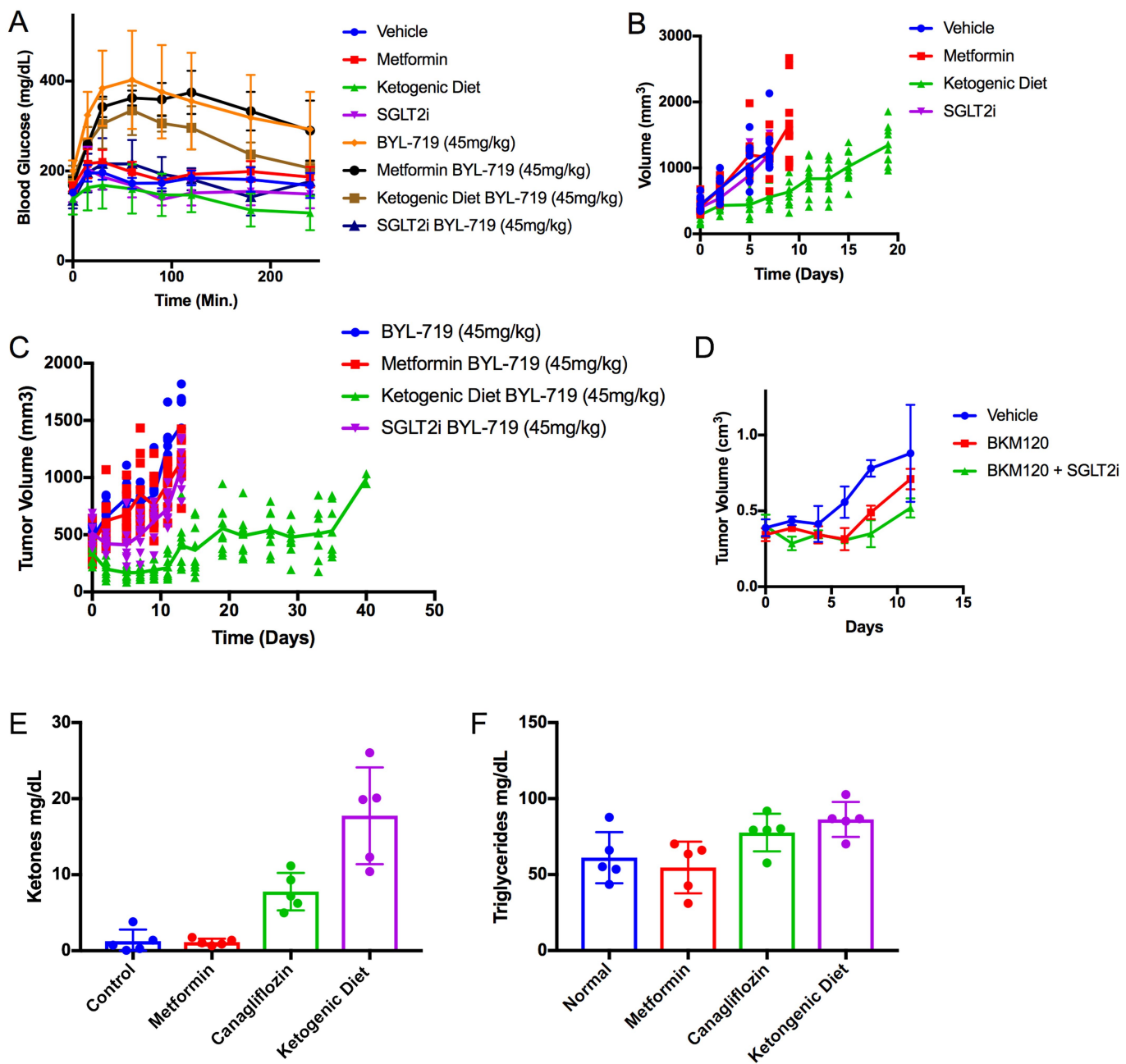
BKM120, GDC-0941, and GDC-0980; $n=4$ for BEZ235; $n=3$ for RAD001. **D**, $n=3$ mice per arm. As a surrogate for total insulin release, c-peptide levels show that the PI3K and IGFR/INSR inhibitors markedly increase insulin release. In all cases, compounds that caused acute increases in blood glucose also increased serum insulin.



Extended Data Fig. 2 | See next page for caption.

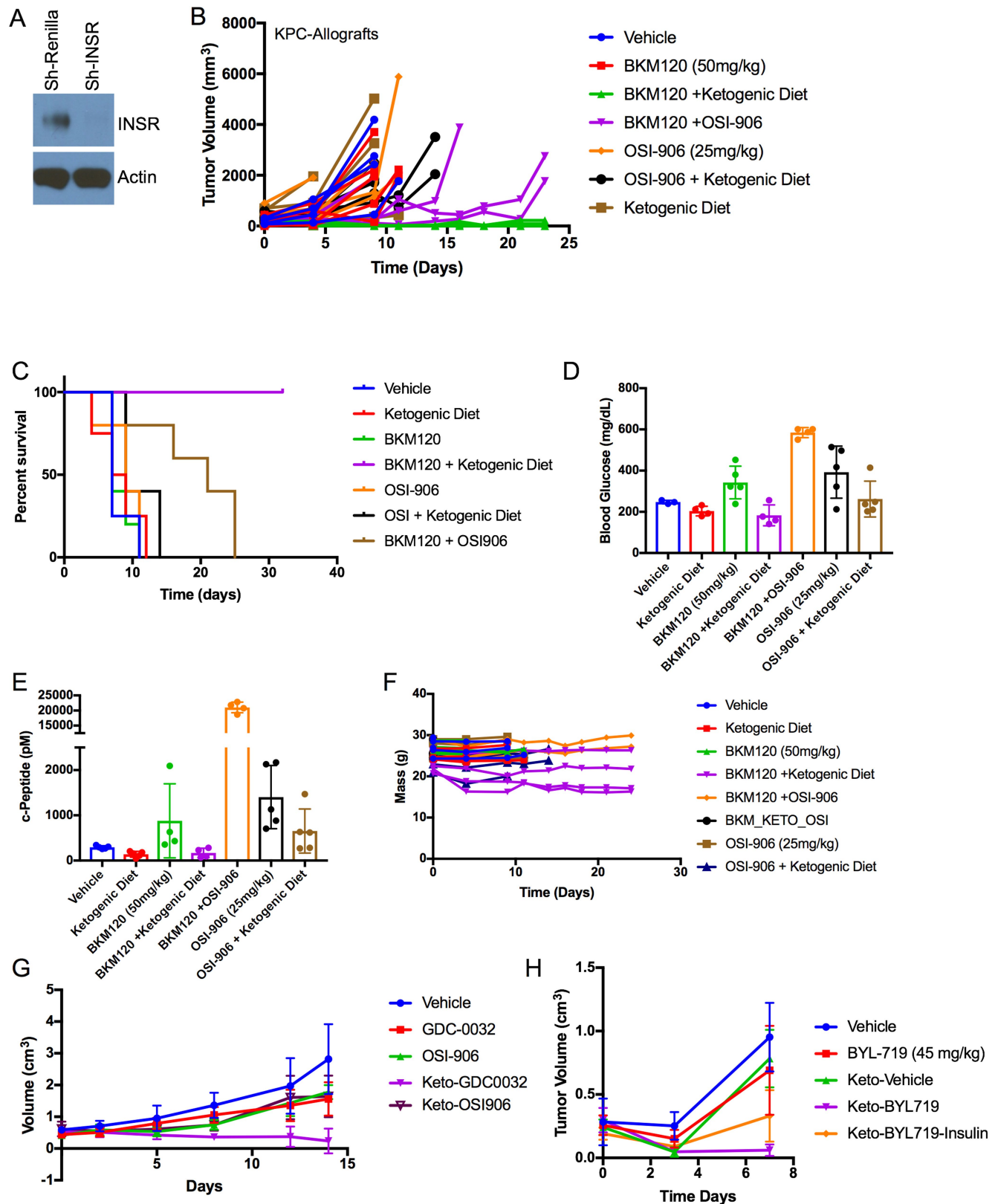
Extended Data Fig. 2 | Effect of feedback levels of insulin observed in Fig. 1 on BKM120 efficacy in vitro. **a**, Proliferation in minimal growth medium of cells whose growth is partially rescued by the addition of the observed feedback levels of insulin (10 ng ml^{-1}) induced by BKM120 in mice. $n = 3$ biologically independent samples per arm, mean \pm s.d. number of cells. **b**, Cell viability assay demonstrating the effects of feedback levels of insulin on two patient-derived organoid cultures (PtA and PtB) being treated in a dose response with BKM120 as measured by cell titre-glo at 96 h. $n = 3$ biologically independent samples per treatment. **c**, Proliferation in minimal growth medium of mouse TNBC cells treated with PI3K inhibitors partially rescued by the addition of the observed feedback levels of insulin induced by BKM120 in mice (Fig. 1). $n = 6$ biologically independent samples per treatment, mean \pm s.d. **d, e**, Proliferation of

HCT116-neo cells (**d**) and HCT116 PTEN knockout (KO) cells (**e**) with and without treatment with physiologically observed levels of insulin (10 ng ml^{-1}) and treatment with the clinically relevant PI3K inhibitors GDC-0032 and BYL-719. $n = 4$ biologically independent samples per treatment, mean \pm s.d. confluence. **f, g**, Proliferation of DLD1-Neo cells (**f**) and DLD-1 PTEN knockout cells (**g**) under the same treatment conditions as in **d** and **e**. Of note, the loss of PTEN in these isogenic sets of colon cancer lines does not uniformly alter the response to insulin in the setting of PI3K inhibition. In the context of PTEN loss, physiological levels of insulin can restore normal proliferation in HCT116 cells despite the presence of PI3K inhibitors. $n = 4$ biologically independent samples per treatment, mean \pm s.d. confluence.



Extended Data Fig. 3 | KPC K8484 allografts treated with PI3K inhibitors with or without supplementary approaches to target systemic insulin feedback. **a**, Mean \pm s.d. blood glucose of mice from Fig. 3e–g treated with control diet, ketogenic diet, metformin (250 mg kg^{-1}), or canagliflozin (SGLT2i; 6 mg kg^{-1}), after the first dose of BYL-719 (45 mg kg^{-1}). $n = 5$ animals per arm. **b**, Volumes of tumours treated with the metabolic modifying agents shown in Fig. 3 without PI3K inhibitors. $n = 10$ tumours per arm for vehicle, metformin, and ketogenic diet; $n = 8$ tumours per arm for SGLT2i. **c**, Mean tumour volumes (lines) with scatter (points) for each of these treatment cohorts. $n = 10$ tumours per arm for

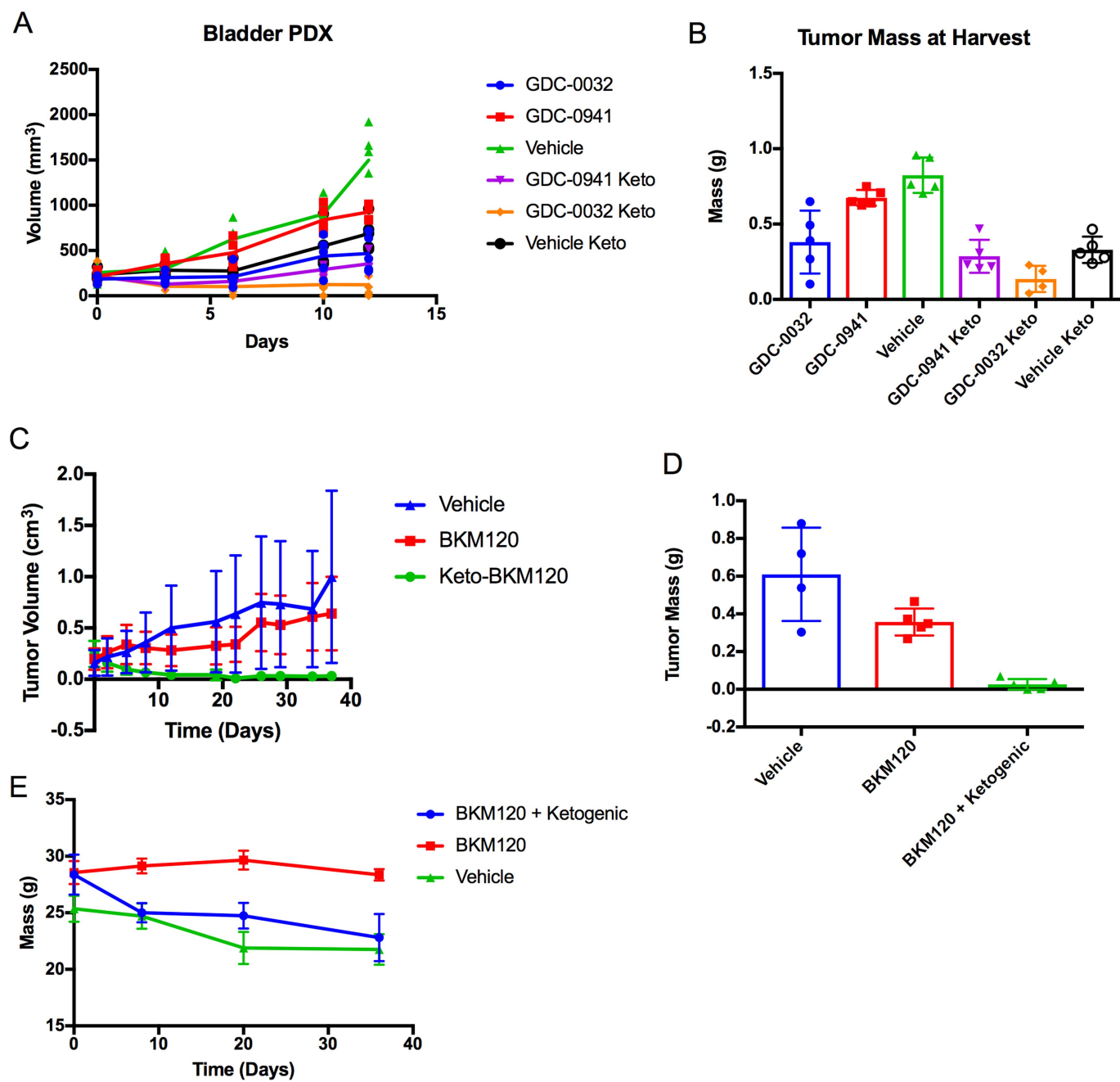
BYL-719, BYL-719 + metformin, and BYL-719 + ketogenic diet; $n = 9$ tumours for BYL-719 + SGLT2i. **d**, Mean \pm s.d. tumour volumes from an independent experiment with mice ($n = 4$ mice per arm) treated daily with BKM120 with or without 6 mg kg^{-1} canagliflozin administered 60 min before PI3K treatment, so that peak SGLT2 inhibition is aligned with peak blood glucose levels after PI3K inhibitor treatment. **e, f**, Mean \pm s.d. blood ketones (e) and triglycerides (f) as determined by calorimetric assay of mice shown in Fig. 3a–d after a single treatment with BKM120 with or without pretreatment with metformin, canagliflozin, or the ketogenic diet. $n = 5$ mice per arm.



Extended Data Fig. 4 | See next page for caption.

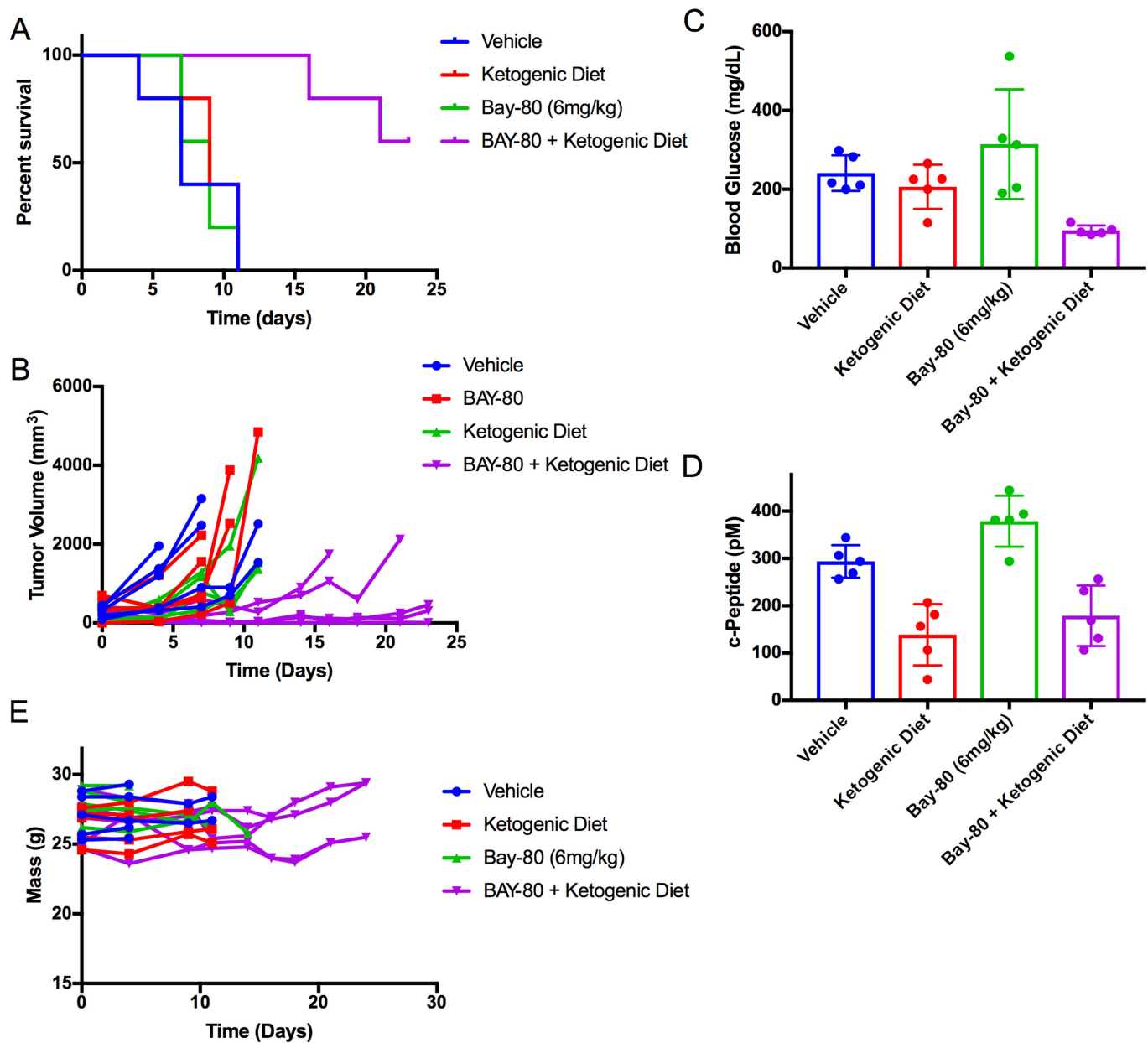
Extended Data Fig. 4 | Role of insulin receptor inhibition in the observed changes in tumour response. **a**, Western blot of cell lysates from K8484 cells used to generate xenografts in Fig. 4a after 36 treatments with doxycycline to induce the shRenilla and shIR hairpins as indicated. Similar results were observed in two independent experiments. **b**, Tumour volumes of individual mice allografted with KPC-K8484 tumours as measured by calipers over time. $n = 4, 5, 4, 4, 5, 5$ and 5 for vehicle, BKM120, BKM120 + ketogenic diet, BKM120 + OSI-906, OSI-906, OSI-906 + ketogenic diet, and ketogenic diet, respectively. **c**, Survival curves of mice in **b**. **d**, **e**, Mean \pm s.d. blood glucose (**d**) and c-peptide (**e**) from these mice 240 min after respective treatments. Two of the glucose measurements in the OSI-906 and BKM120 were beyond the range of the detector ($>600 \text{ mg dl}^{-1}$). **f**, Masses of individual mice over the course of treatment. As has been previously published, mice lose 10–20% of

their mass upon initiation of a ketogenic diet²⁹. **g**, Similar to the data for the tumours in **a**, both OSI-906, a INSR/IGFR inhibitor, and GDC-0032 showed greater anti-tumour efficacy in PIK3CA + MYC mutant mouse breast tumour allografts, ES-278, grown in wild-type *c57/bl6* mice fed a ketogenic diet. $n = 5$ tumours per arm. Points depict mean \pm s.d. tumour volume. **h**, Mean \pm s.d. tumour volumes of wild-type *c57/bl6* mice bearing KPC allografted tumours as measured by calipers over time. Mice were treated as indicated with combinations of BYL-719, the ketogenic diet, or insulin as in Fig. 4b. Mice in the ketogenic + BYL719 + insulin cohort lost $>20\%$ of their body mass over the 1 week of treatment so the experiment was terminated at day 7. $n = 6, 4, 4, 6, 6$ for vehicle, BYL-719, ketogenic diet, BYL-719 + ketogenic diet, and BYL-719 + ketogenic diet + insulin, respectively.



Extended Data Fig. 5 | Effect of PI3K inhibitor treatments on PDX model of bladder cancer and syngeneic allograft models of PIK3CA mutant breast cancer. **a**, Graph of tumour growth over time of a PDX from a patient with bladder cancer (Patient C) treated with the pan-PI3K inhibitor GDC-0941 or the β -sparing inhibitor GDC-0032, alone or with a ketogenic diet. Lines indicate mean tumour volume of each treatment group, points indicate individual tumour volumes over time. $n=5$

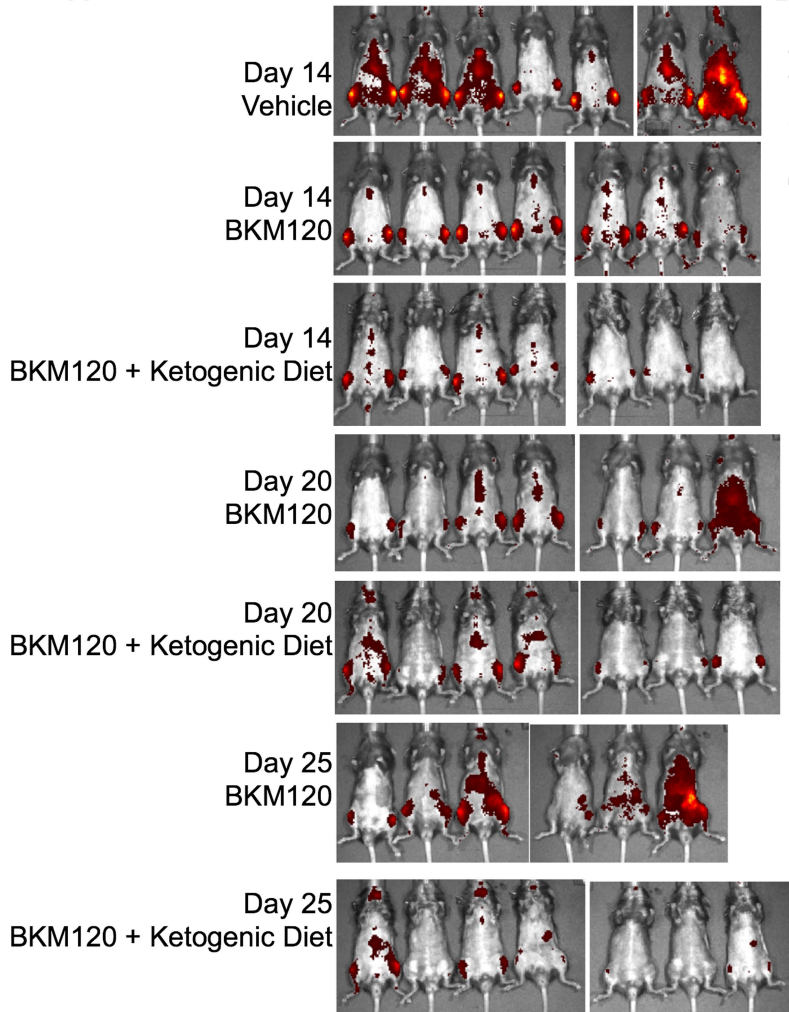
tumours per arm. **b**, Mean \pm s.d. tumour mass at the time of removal on day 12. **c, d**, Mean \pm s.d. tumour growth over time (**c**) and tumour mass at time of removal (**d**) from mice with orthotopic allografts of a PIK3CA (H1047R) mutant mouse breast cancer, ES272, treated as indicated with BKM120 alone or in combination with a ketogenic diet. $n=4, 5, 5$ tumours per arm for vehicle, BKM120 and BKM120 + ketogenic diet, respectively. **e**, Mean \pm s.d. mass of mice over time.



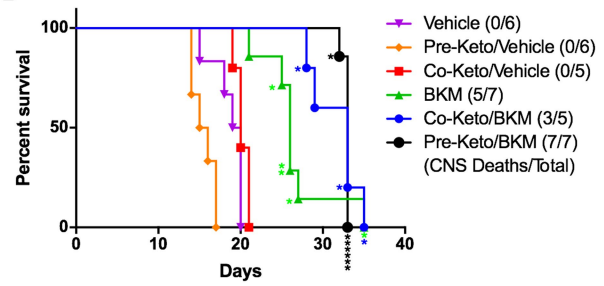
Extended Data Fig. 6 | Effect of copanilisib with or without ketogenic diet on growth of KPC tumour model K8082 grown in the flank of wild-type *c57/bl6* mice. **a**, Survival curves for mice with KPC K8082 allografts grown in the flank and treated as indicated with BAY 80-6946 alone or combined with pretreatment with a ketogenic diet as indicated (*P* value comparing BAY 80-6946 with the combination of BAY 80-6946 with ketogenic diet was 0.0019 by Mantel–Cox log-rank test). *n* = 5 mice

per arm for vehicle, BAY 80-6946, and BAY 80-6946 + ketogenic diet; *n* = 4 for ketogenic diet alone. **b**, Volume of each tumour in this cohort plotted individually. **c, d**, Mean \pm s.d. blood glucose (**c**) and c-peptide (**d**) in mice in **b, c**, 240 min after treatment. **e**, Mass of these mice over time on treatment. Tumours were allowed to grow until their diameters were >0.6 cm before the initiation of treatment.

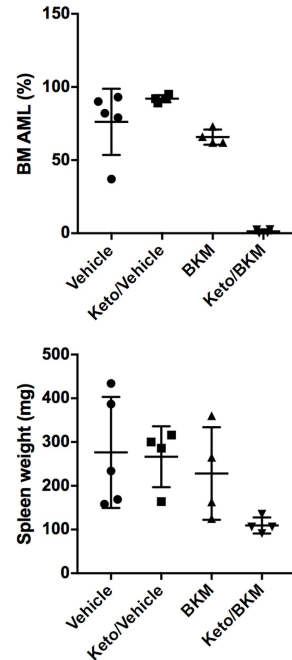
A



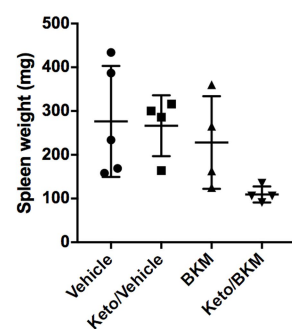
B



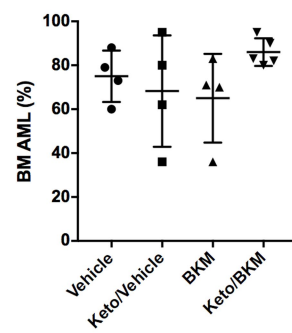
C



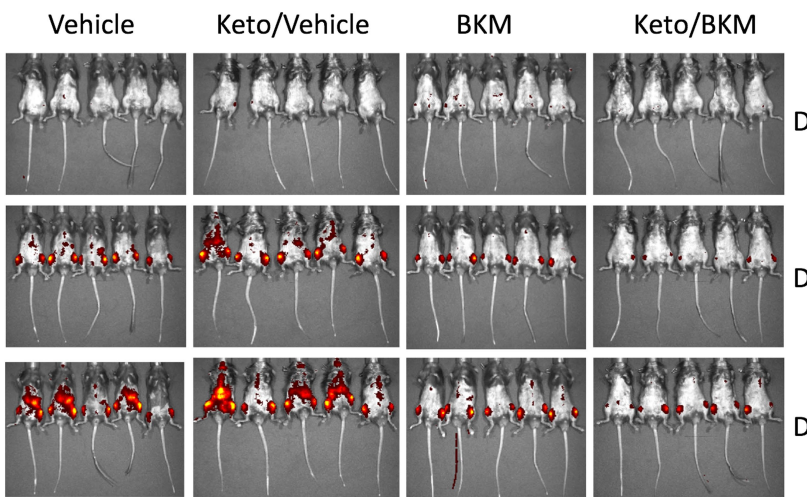
D



E



F



Extended Data Fig. 7 | See next page for caption.

Extended Data Fig. 7 | Effect of BKM120 + ketogenic diet on a syngeneic model of AML. **a**, IVIS images of AML burden (as reported by DS-red) in over time. The group labelled BKM120 plus ketogenic diet were pre-treated with a ketogenic diet. $n = 7$ mice per arm. **b**, Survival curves of mice from a with additional mice to evaluate pre-treatment versus co-treatment with the ketogenic diet in the syngeneic model of AML treated with BKM120 alone or in combination with a ketogenic diet. Individual lines are shown for initiation of ketogenic diet before (pre) or at the same time as the initiation of BKM120 treatment (co); in both cases, BKM120 efficacy is significantly enhanced by the addition of the ketogenic diet ($P = 0.0142$ and 0.0316 by Gehan–Breslow Wilcoxon test for pre and co compared to BKM alone, respectively). *Mice that were euthanized owing to paralysis resulting from AML infiltrating the CNS, rather than deaths typically seen in these mice due to tumour burden. Of note, the mice in the BKM + ketogenic diet group were frequently euthanized due to paralysis, but this was not frequently a cause of mortality in the other treatment

groups. $n = 6, 6, 5, 7, 5, 7$ mice per arm for vehicle, pre-ketogenic diet, co-ketogenic diet, BKM120, co-ketogenic diet + BKM120, and pre-ketogenic diet + BKM120, respectively. **c, d**, Disease burden of AML as measured by per cent DS-red positive AML cells in bone marrow (c) and spleen weight across the treatment groups (**D**) (pre-treated with ketogenic diet). Data are mean \pm s.d. $n = 5, 4, 4, 4$ mice per arm for vehicle, pre-ketogenic diet, BKM120, and pre-ketogenic diet + BKM120, respectively. **e**, Measurement of AML burden in mice that were pretreated with BKM120 and/or a ketogenic diet to demonstrate that the effects observed in the AML studies are not the result of implantation issues related to the pretreatment. Data are mean \pm s.d. $n = 4, 4, 4, 5$ mice per arm for vehicle, pre-ketogenic diet, BKM120, and pre-ketogenic diet + BKM120, respectively. **f**, Images of mice treated as indicated with BKM120 and ketogenic diet where the diet and BKM120 therapy were initiated on the same day (co-treatment). $n = 5$ mice per arm.

Reporting Summary

Nature Research wishes to improve the reproducibility of the work that we publish. This form provides structure for consistency and transparency in reporting. For further information on Nature Research policies, see [Authors & Referees](#) and the [Editorial Policy Checklist](#).

Statistical parameters

When statistical analyses are reported, confirm that the following items are present in the relevant location (e.g. figure legend, table legend, main text, or Methods section).

n/a	Confirmed
<input type="checkbox"/>	<input checked="" type="checkbox"/> The exact sample size (n) for each experimental group/condition, given as a discrete number and unit of measurement
<input type="checkbox"/>	<input checked="" type="checkbox"/> An indication of whether measurements were taken from distinct samples or whether the same sample was measured repeatedly
<input type="checkbox"/>	<input checked="" type="checkbox"/> The statistical test(s) used AND whether they are one- or two-sided <i>Only common tests should be described solely by name; describe more complex techniques in the Methods section.</i>
<input type="checkbox"/>	<input checked="" type="checkbox"/> A description of all covariates tested
<input type="checkbox"/>	<input checked="" type="checkbox"/> A description of any assumptions or corrections, such as tests of normality and adjustment for multiple comparisons
<input type="checkbox"/>	<input checked="" type="checkbox"/> A full description of the statistics including central tendency (e.g. means) or other basic estimates (e.g. regression coefficient) AND variation (e.g. standard deviation) or associated estimates of uncertainty (e.g. confidence intervals)
<input checked="" type="checkbox"/>	<input type="checkbox"/> For null hypothesis testing, the test statistic (e.g. F , t , r) with confidence intervals, effect sizes, degrees of freedom and P value noted <i>Give P values as exact values whenever suitable.</i>
<input checked="" type="checkbox"/>	<input type="checkbox"/> For Bayesian analysis, information on the choice of priors and Markov chain Monte Carlo settings
<input checked="" type="checkbox"/>	<input type="checkbox"/> For hierarchical and complex designs, identification of the appropriate level for tests and full reporting of outcomes
<input checked="" type="checkbox"/>	<input type="checkbox"/> Estimates of effect sizes (e.g. Cohen's d , Pearson's r), indicating how they were calculated
<input type="checkbox"/>	<input checked="" type="checkbox"/> Clearly defined error bars <i>State explicitly what error bars represent (e.g. SD, SE, CI)</i>

Our web collection on [statistics for biologists](#) may be useful.

Software and code

Policy information about [availability of computer code](#)

Data collection

Cell Proliferation data was collected using Incucyte Software. Living Image 4.5 was used for in vivo imaging. ASIPro VMTM software was used for PET

Data analysis

Prism7 Software was used for statistical analysis. LivingImage4.5 was used for image quantification in vivo modeling. ASIPro VMTM software was used for PET analysis. Incucyte was utilized for cell proliferation assays.

For manuscripts utilizing custom algorithms or software that are central to the research but not yet described in published literature, software must be made available to editors/reviewers upon request. We strongly encourage code deposition in a community repository (e.g. GitHub). See the Nature Research [guidelines for submitting code & software](#) for further information.

Data

Policy information about [availability of data](#)

All manuscripts must include a [data availability statement](#). This statement should provide the following information, where applicable:

- Accession codes, unique identifiers, or web links for publicly available datasets
- A list of figures that have associated raw data
- A description of any restrictions on data availability

Data availability: Source data for figures 1,3 and 4 as well as Extended figures 1,3-7 are provided in the online version of the paper.

Field-specific reporting

Please select the best fit for your research. If you are not sure, read the appropriate sections before making your selection.

Life sciences

Behavioural & social sciences Ecological, evolutionary & environmental sciences

For a reference copy of the document with all sections, see nature.com/authors/policies/ReportingSummary-flat.pdf

Life sciences study design

All studies must disclose on these points even when the disclosure is negative.

Sample size	Sample sizes were chosen based upon previous experience with the animal models. Or following convention of the methods. No power analysis was preformed for the design of these studies.
Data exclusions	No completed data were excluded from the experiments presented in this manuscript.
Replication	Data described in this manuscript were reliably reproduced. The PET imaging in figure one was only run twice and though similar observations were made visually there was a problem with the quantification due to a failure of the CT.
Randomization	As the diet arms needed to be kept together so that the animal feed for each group could be controlled, cages were randomized to treatment groups rather than individual mice. Randomization occurred before tumor implantation.
Blinding	No blinding was used in these studies. The mouse diets prevented effective blinding of the animal work. Due to the composition of the ketogenic diet blinding was not possible for our animal studies as mice on different diets are readily identified.

Reporting for specific materials, systems and methods

Materials & experimental systems

n/a	Involved in the study
<input checked="" type="checkbox"/>	<input type="checkbox"/> Unique biological materials
<input type="checkbox"/>	<input checked="" type="checkbox"/> Antibodies
<input type="checkbox"/>	<input checked="" type="checkbox"/> Eukaryotic cell lines
<input checked="" type="checkbox"/>	<input type="checkbox"/> Palaeontology
<input type="checkbox"/>	<input checked="" type="checkbox"/> Animals and other organisms
<input checked="" type="checkbox"/>	<input type="checkbox"/> Human research participants

Methods

n/a	Involved in the study
<input checked="" type="checkbox"/>	<input type="checkbox"/> ChIP-seq
<input checked="" type="checkbox"/>	<input type="checkbox"/> Flow cytometry
<input checked="" type="checkbox"/>	<input type="checkbox"/> MRI-based neuroimaging

Antibodies

Antibodies used

All of the antibodies used for western blotting have been extensively used in the literature for previous studies, and validation blots are shown in the product information sheets on the Cell Signaling or Abcam Websites.
 pINSR CST 3024S 15 1:1000
 INSR CST #3025 8 1:1000
 pAKT308 CST 9275L 5 1:1000
 pAKT473 CST 9271S 14 1:1000
 AKT CST 4691S 20 1:1000
 pERK CST 9101S 29 1:1000
 ERK CST 4695S 26 1:1000
 pS6 CST 2215S 14 1:1000
 S6 CST 2217S 7 1:1000
 Actin Abcam ab6276 gr3185620-12 1:10000

IHC staining was validated and scored by a pathologist using the antibodies at the dilutions below.
 Ki67 (Abcam, ab16667) 1:500; cleaved caspase-3 (Asp175; 5A1E; Cell Signaling Technology, 9664) 1:200; phospho-INSR (Tyr 1162; Thermo Fisher #AHR0271) 1:100; phospho-AKT (Ser473; Cell Signaling Technology, 8101) 1:20; and phospho-S6 ribosomal protein (Ser235/236; Cell Signaling Technology, 2211) 1:300)

Validation

All of the antibodies used for western blotting have been extensively used in the literature for previous studies, and validation blots are shown in the product information sheets on the Cell Signaling or Abcam Website. IHC staining was validated and scored by a pathologist using the antibodies listed above.

Eukaryotic cell lines

Policy information about [cell lines](#)

Cell line source(s)

Cell lines were acquired from ATCC, or were provided for academic use from laboratories at Columbia University. Specifically The murine KPC cell lines came from the laboratory of Kenneth Olive. The AML cell lines from the lab of Siddhartha Mukherjee. Isogenic HCT116 and DLD-1 lines were obtained from Todd Waldman at Georgetown University.

Authentication

Human Cell lines were purchased from ATCC. No authentication was possible for the murine derived lines.

Mycoplasma contamination

Cell Lines tested negative for mycoplasma contamination.

Commonly misidentified lines
(See [ICLAC](#) register)

None of the cell lines in this paper are on the ICLAC list of commonly misidentified cell lines.

Animals and other organisms

Policy information about [studies involving animals; ARRIVE guidelines](#) recommended for reporting animal research

Laboratory animals

PDX studies were performed in female nude (inbred) mice from Jackson Labs (Foxn1 Nu). Allograft studies were performed using C57BL/6J mice also from Jackson Labs. Allograft studies were conducted using both male and female mice, though they were not mixed within experiments. Mice were implanted at 8-12 weeks of age (age matched per study). Typically C57 Male mice in these cohorts weighed between 24-30 grams. While C57 female mice weighed between 22-28 grams. Nude were typically 18-24 grams at time of tumor implantation.

Wild animals

No wild animals were used in these studies.

Field-collected samples

No field collected samples were used in these studies.